Microtubule-targeting agents augment the toxicity of DNA-damaging agents by disrupting intracellular trafficking of DNA repair proteins

Marianne S. Poruchynsky[a,1], Edina Komlodi-Pasztor[a,1], Shana Trostel[a], Julia Wilkerson[a], Marie Regairaz[b,2], Yves Pommier[b], Xu Zhang[a], Tapan Kumar Maity[a], Robert Robey[b], Mauricio Burotto[a], Dan Sackett[c], Udayan Guha[a], and Antonio Tito Fojo[a,3]

[a]Center for Cancer Research, National Cancer Institute, [b]Developmental Therapeutics Branch, National Cancer Institute, and [c]Program in Physical Biology, Eunice Kennedy Shriver National Institute of Child Health and Human Development, National Institutes of Health, Bethesda, MD 20892

The paradigm that microtubule-targeting agents (MTAs) cause cell death via mitotic arrest applies to rapidly dividing cells but cannot explain MTA activity in slowly growing human cancers. Many preferred cancer regimens combine a MTA with a DNA-damaging agent (DDA). We hypothesized that MTAs synergize with DDAs by interfering with trafficking of DNA repair proteins on interphase microtubules. We investigated nine proteins involved in DNA repair: ATM, ATR, DNA-PK, Rad50, Mre11, p95/NBS1, p53, 53BP1, and p63. The proteins were sequestered in the cytoplasm by vincristine and paclitaxel but not by an aurora kinase inhibitor, colocalized with tubulin by confocal microscopy and coimmunoprecipitated with the microtubule motor dynein. Furthermore, adding MTAs to radiation, doxorubicin, or etoposide led to more sustained γ-H2AX levels. We conclude DNA damage-repair proteins traffic on microtubules and addition of MTAs sequesters them in the cytoplasm, explaining why MTA/DDA combinations are common anticancer regimens.

microtubule targeting agents | DNA-damaging agents | combination chemotherapy | targeted therapies | DNA repair protein trafficking

First developed as anticancer agents in the 1950s, microtubule targeting agents (MTAs) are used in the treatment of a wide variety of malignancies and until now have been thought to kill cells by arresting them in mitosis (1, 2). Although this explanation applies to rapidly dividing cells in preclinical models, it cannot explain the activity of these agents in tumors in humans because these cells divide much more slowly. For the latter situation, a different paradigm must explain the activity of MTAs, and we have proposed that interfering with microtubule (MT) trafficking in interphase cells is the principal mechanism of MTA action (3–5). In breast, ovarian, lung, and head and neck cancers, as well as in most lymphomas, combination regimens that include a MTA and a DNA-damaging agent (DDA) are preferred (Table S1). Although the frequency with which these combinations are used might be fortuitous, it is likely there is a mechanistic basis for this outcome. We hypothesized that by hampering the trafficking of essential DNA repair proteins, MTAs synergize with DDAs, augmenting their toxicity. To explore this theory further we studied the effects of combining a MTA and a DDA in a number of cell models and examined the distribution and biology of nine different proteins involved in DNA repair. We have confirmed the hypothesis and report our findings.

Results

Vincristine Increases Cytoplasmic Retention of Eight DNA Damage-Repair Proteins in A549 Cells.
We began by testing our hypothesis that proteins involved in the repair of DNA damage traffic from the cytoplasm to the nucleus on MTs. If true, one would expect treatment with a MTA, such as vincristine, to affect their

intracellular distribution. In these and all other experiments we chose noncytotoxic drug concentrations, allowing us to examine viable cells. We examined eight proteins that repair DNA damage (ATM, ATR, DNA-PK, Rad50, Mre11, p95NBS1, p53, and 53BP1), choosing them from a larger number initially considered based on the availability of commercial antibodies that performed well on immunoblots and immunofluorescence in A549 cells. We treated A549 cells with vincristine or doxorubicin alone or in combination, and examined the intracellular distribution of the eight proteins both in the absence of any DNA damage or after doxorubicin-induced DNA damage (primarily to induce p53 levels), cognizant that all of these proteins might not be involved in the repair of doxorubicin-induced DNA damage. As shown in Fig. 1, for all eight proteins, the percentage in the cytoplasm was greater in cells treated with either vincristine alone or vincristine in combination with doxorubicin, compared with those treated only with doxorubicin or not treated at all. The fold-increase in cytoplasmic retention was consistently approximately two- to sevenfold, confirming a role for MTs in the

Significance

Drugs targeting microtubules are among the most active anti-cancer agents. In vitro and in preclinical models, these agents are said to interfere with mitosis. However human tumors divide too slowly for this paradigm to apply, evidenced by the failure of over a dozen well-designed antimitotic agents targeting the aurora kinases and kinesin spindle protein that had minimal antitumor activity but caused severe bone marrow suppression. We have proposed that microtubule-targeting agents interfere with the trafficking of critical proteins in interphase microtubules. If true, then one must identify critical proteins whose traffic on microtubules is impacted. We identify nine DNA repair proteins that traffic on microtubules, explaining why combinations of a microtubule-targeting agent and a DNA-damaging agent are frequently used in cancer therapy.
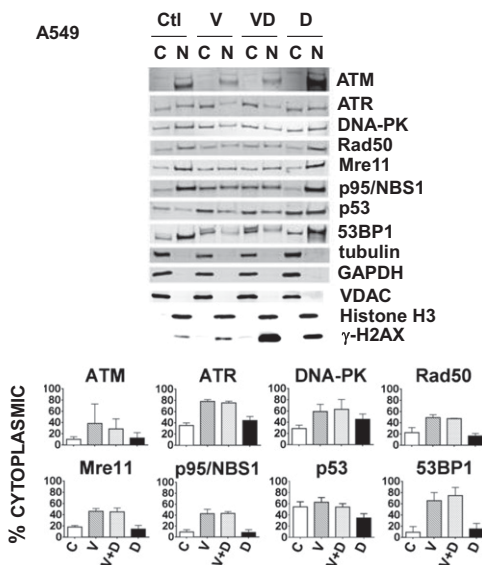
MEDICAL SCIENCES

Fig. 1. Treatment of A549 cells with the MTA vincristine, alone or in combination with a DNA-damaging agent, doxorubicin, causes increased cytoplasmic retention of the DNA damage-repair proteins ATM, ATR, DNA-PK, Rad50, Mre11, p95/NBS1, p53, and 53BP1. A549 cells were untreated (Ctl), or treated either with 200 nM vincristine (V) for 24 h or 400 ng/mL doxorubicin (D) for 4 h, either separately or in combination (V for 20 h followed by V+D for an additional 4 h). Cytoplasmic (C) and nuclear (N) fractions prepared as described in *Materials and Methods*, are indicated for Western blots probed with antibodies against the repair proteins and five fractionation controls (tubulin, GAPDH, VDAC, Histone H3, or γ-H2AX). The percentage of protein in the C fraction is indicated and calculated as: [C/(C+N)] × 100%. Means and SDs are shown. The number of experiments (n) were: ATM (three), ATR (three), DNA-PK (three), Rad50 (three), Mre11 (three), p95/NBS1 (three), p53 (six), and 53BP1 (four). For the proteins studied, drug treatment had no or very little effect on their amount as shown in the blots of lysates seen in Fig. 4 and Fig. S3. Because no protein is lost in the fractionation procedure, all proteins appear in either the N or the C fraction, and the percent in each fraction can be accurately calculated from the results of the immunoblot.

trafficking of DNA damage-repair proteins to the nucleus and demonstrating the vulnerability of this transport process to a MTA. Similar results were obtained in four nonadherent Burkitt's lymphoma cell lines (CA46, DG-75, Ramos, and ST486) with increased cytoplasmic retention of 53BP1 observed with vincristine plus doxorubicin or vincristine alone, compared with doxorubicin-treated cells or the untreated control (Fig. S1).

Neither the Aurora Kinase Inhibitor, VX680, Nor Serum Starvation Affect the Cellular Distribution of DNA Damage-Repair Proteins. To confirm that the increase in cytoplasmic retention of DNA damage-repair proteins after treatment with a MTA was a result of impaired MT trafficking and not mitotic arrest or possibly nuclear membrane disruption, we conducted the additional experiments shown in Fig. 2. We (*i*) treated A549 cells with the aurora kinase inhibitor (AKI), VX680, and (*ii*) serum-starved SKOV3 cells to reduce the fraction of cells arresting in mitosis after vincristine. As shown in Fig. 2*A*, compared with control cells, both VX680 and vincristine induced similar G_2M arrest, allowing us to address the effect of cell cycle arrest on the cellular distribution of the proteins. As shown in Fig. 2*B* and tabulated below the figure, compared with vincristine, VX680 had no effect on the cellular distribution of the eight proteins, excluding the possibility of cell cycle arrest as the etiology of the altered cellular distribution and supporting interference of protein trafficking on MTs as the cause of cytoplasmic sequestration. Similar results are shown in a separate experiment in Fig. 2*C* and these are compared with the effect of another MTA,

paclitaxel. As in Fig. 2*B*, VX680 (AKI) has no effect on the nuclear/cytoplasmic distribution, whereas paclitaxel, like vincristine, resulted in increased cytoplasmic retention of several DNA damage-repair proteins. Additionally, we compared the cellular distribution of the DNA damage-repair proteins in SKOV3 cells that either were treated with serum or deprived of serum for 48 h,
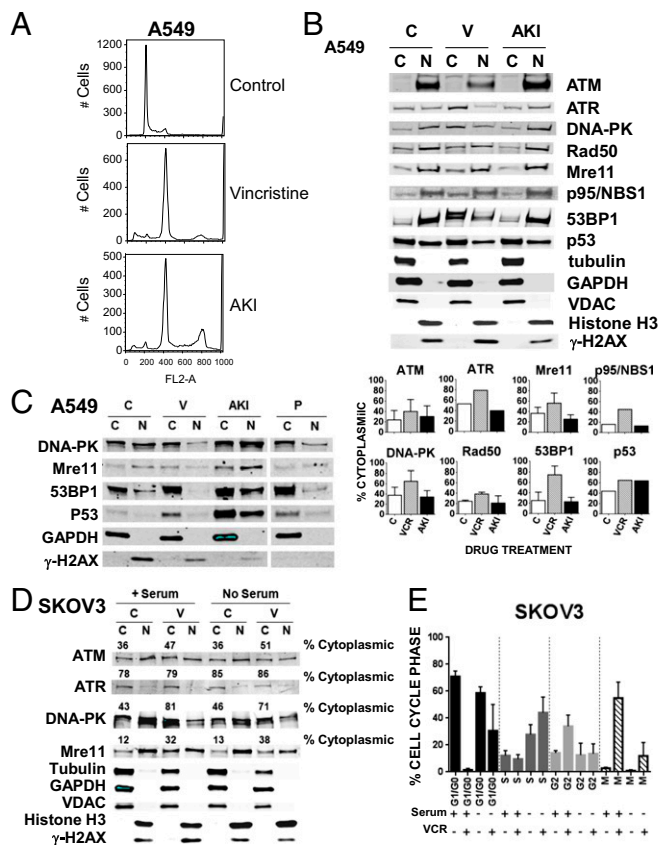

Fig. 2. Treatment of A549 cells with the AKI VX680 fails to increase cytoplasmic accumulation of the DNA damage-repair proteins. (*A*) A549 cells were untreated (C, control) or treated with either 200 nM vincristine (V) or 250 nM of the AKI VX-680 (Tozasertib) for 24 h. Cells were further processed for flow cytometry as described. (*B*) A549 lysates treated as described in *A* were prepared and separated into cytoplasmic (C) and nuclear (N) fractions as described in *Materials and Methods*. Western blots were probed with antibodies as in Fig. 1. The percent of the protein in the C fraction is indicated and calculated as: [C/(C+N)] × 100%. Means and SDs are shown. The number of experiments (n) were: ATM (four), Mre11 (three), DNA-PK (three), Rad50 (two), and 53BP1 (four). Because p53 is wild-type in A549 cells and expressed at very low levels in the absence of drug treatment (see p53 Western blot in Fig. 1), the sample shown under the "C" control designation was treated with 400 ng/mL doxorubicin (D) for 4 h and serves as comparison for samples alongside those treated with either 250 nM of AKI for 24 h or 200 nM V for 24 h followed by a V + D combination for an additional 4 h. (*C*) A549 cells were treated as in *A* or also with 200 nM paclitaxel (P) for 24 h before being separated into "C" and "N" fractions. (*D*) SKOV3 cells incubated with or without serum for 48 h were then treated or not with 100 nM V with or without serum for another 24 h. C and N fractions were prepared as described in *Materials and Methods*. Western blots were probed with four antibodies that performed well with SKOV3 cell extracts: ATM, ATR, DNA-PK, and Mre11, and also with antibodies for tubulin, GAPDH, VDAC, Histone H3, and γ-H2AX. The percentage of protein in the C fraction is indicated and calculated as [C/(C+N)] × 100%. (*E*) SKOV3 cells treated as described in *D* were further processed for flow cytometry, and mitotic cells were quantitated by two-variable analysis, as described in *Materials and Methods*. The percentage of cells in each phase of the cell cycle (G_1/G_0, S, G_2, or M) is indicated for the different treatments. The mean and error bars display data compiled from three experiments.

the latter to slow transition through the cell cycle before treatment with vincristine. We chose SKOV3 cells because their course through the cell cycle can be slowed by serum starvation (6). As shown in Fig. 2D, with or without serum we observed similar cytoplasmic/nuclear distribution before and after vincristine for four DNA damage-repair proteins that could be reliably detected with our antibodies in the SKOV3 cells. The distributions were similar despite fewer cells in mitosis in serum-starved cells (Fig. 2E), indicating the outcome was independent of the fraction of cells in mitosis. In these as in all experiments, distribution of all cytoplasmic and nuclear marker proteins were unaffected by alterations in cell cycle phases and indicate the lack of measurable contamination of the fractions.

Immunofluorescence Demonstrates Colocalization of DNA Damage-Repair Proteins and MTs. To provide additional evidence for an interaction between the DNA damage-repair proteins and MTs, we performed confocal microscopy on untreated A549 cells fixed and incubated with antibodies to one of the DNA damage-repair proteins followed by an antitubulin antibody. As shown in Fig. 3, colocalization with MTs was observed for DNA-PK, p95NBS1, Mre11, 53BP1, p53, and p63 proteins, often seen to be linear and punctate along MTs; and except for p63, the proteins also localized prominently to nuclei. Antibodies against ATM and ATR did not perform well by immunofluorescence, precluding definitive conclusions. This association occurs only with intact MTs and not soluble tubulin (after vincristine treatment) nor the MT bundles that occur following paclitaxel (results with DNA-PK, Mre11, 53BP1, and p53 after vincristine and paclitaxel are shown in Fig. S2). Additionally, gelsolin, used as a control protein that neither associates with nor traffics on MTs and does not appear in the nucleus, localized to actin and the cytoplasm and had neither MT nor nuclear localization (Fig. S2).

DNA Damage-Repair Proteins Coimmunoprecipitate with Dynein. Next we asked whether an antibody against the MT motor protein dynein could coimmunoprecipitate the DNA damage-repair proteins. As shown in Fig. 4, we observed specific variable coimmunoprecipitation of the eight DNA damage-repair proteins with dynein both in the absence of any drug and after treatment of A549 cells with doxorubicin or vincristine. The dynein immunoprecipitation depleted dynein but did not deplete Mre11 or ATM, indicating only a small fraction of these proteins is associated with dynein at any given time (Fig. S3). The latter finding is consistent with the experiments showing prominent fractionation/localization of these DNA repair proteins in the nucleus, where they have primary functions. Additionally, consistent with this, reciprocal coimmunoprecipitations did not in most cases precipitate dynein because only a small fraction of each DNA repair protein is bound to dynein at any one time (Fig. S3). These results further support the hypothesis that trafficking of DNA damage-repair proteins on MTs could be susceptible to MTAs.

Paclitaxel Treatment Results in Higher and Sustained Levels of γ-H2AX Protein in A549 and MCF7 Cells Treated with Radiation. To further investigate the relationship between the repair of damaged DNA and MT integrity, we asked if a MTA could prolong the effect of DNA damage caused by radiation. To do this, we quantitated the levels of γ-H2AX, a phosphorylated form of H2AX considered an indicator of DNA damage, in A549 and MCF7 cells pretreated with 200 nM paclitaxel and irradiated with 10 Gy. As shown in Fig. 5, in control cells treated with only radiation, the levels of γ-H2AX had fallen substantially by 2 h and had nearly disappeared at 4 h. However, in cells treated with paclitaxel, γ-H2AX levels remained high, with substantial amounts of γ-H2AX still present at 4 and 8 h. This finding further confirmed the hypothesis that DNA damage-repair proteins traffic to the nucleus on MTs and that transport is hampered by MTAs.

Vincristine Results in Higher and Sustained γ-H2AX Levels in MCF7 and A549 Cells Treated with a DNA-Damaging Agent. To assess the effects of MT disruption on drug-induced DNA damage, MCF7 and A549 cells were incubated in vincristine for 20–24 h before a 4-h incubation in vincristine plus either of two DDAs, 200 ng/mL
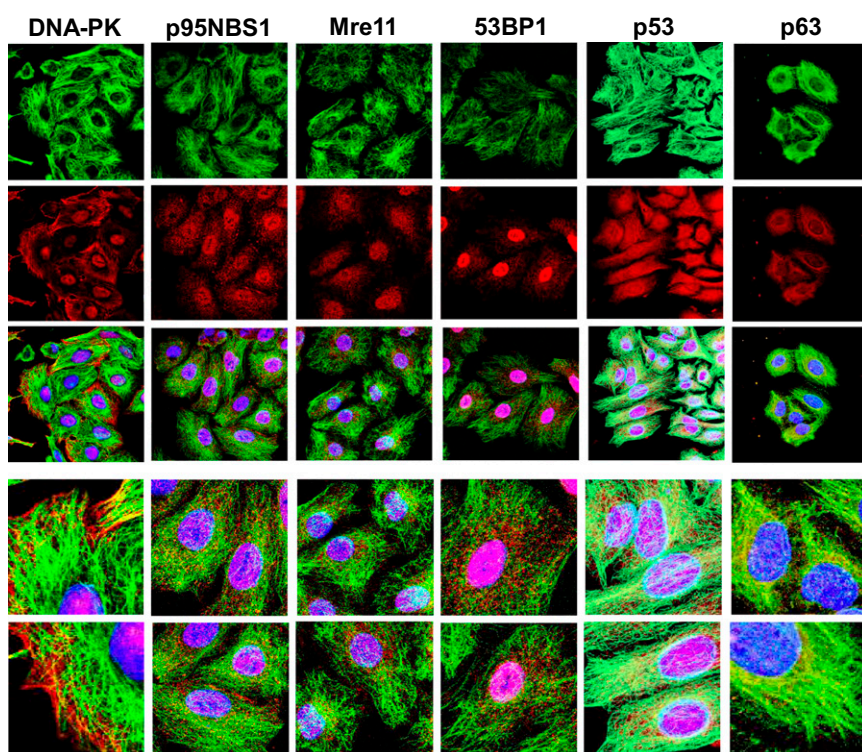

Fig. 3. DNA damage-repair proteins colocalize with MTs as visualized by immunofluorescence microscopy. Confocal immunofluroescent localization of DNA damage-repair proteins (DNA-PK, p95NBS1, Mre11, 53BP1, p53, or p63) and tubulin in A549 cells. Tubulin (FITC-conjugated secondary antibody, green); DNA repair proteins (RHOD-conjugated secondary antibody, red); DAPI stain (blue) localizes to cell nuclei. The tricolor localization of "Tubulin/DNA-damage-repair-protein/DAPI" is shown by the superimposition of three confocal images in the third panel down in each column. Enlarged areas from these images are displayed in the bottom two panels of each column. Images are shown as 3D maximal projections reconstructed from z-stacks or a single slice of a projection. (Magnification in each column: top three images, 630×; lower two images, 2500×.)
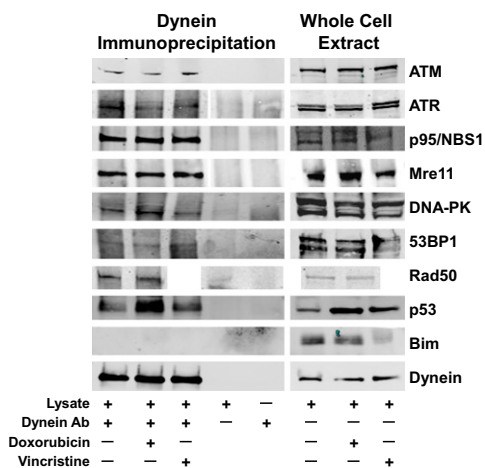
Fig. 4. DNA damage-repair proteins coimmunoprecipitate with the MT motor protein dynein. A549 cells either untreated, treated with 100 nM vincristine overnight, or 400 ng/mL doxorubicin for 4 h, were lysed in immunoprecipitation buffer, homogenized and incubated overnight with an anti-dynein antibody. Whole-cell extracts (50-μg aliquots) or dynein immunoprecipitation samples (the entire immunoprecipitation harvest from 1 mg of whole-cell protein) were resolved by SDS/PAGE, and the Western blots were probed with antibodies to the DNA repair proteins ATM, ATR, P95/NBS1, Mre11, DNA-PK, 53BP1, and p53, Rad50 (no vincristine-treated sample), the control protein Bim, or dynein. The extent of coimmunoprecipitation varies for each protein.

doxorubicin or 4 μM etoposide. Subsequently, the DDA was removed but the cells were maintained in vincristine for an additional 1, 2, 4, 6, or 8 h to monitor the levels and rate of disappearance of γ-H2AX. Control cells were treated similarly with the DDA but did not receive vincristine. As in the preceding experiments with paclitaxel and radiation, Figs. 6 and 7 show that vincristine resulted in γ-H2AX levels that were maintained above basal levels longer compared with the results in control cells treated only with the DDA for 4 h. Thus, again, disruption of MTs, this time using vincristine instead of paclitaxel, resulted in more sustained DNA damage, supporting the necessity for intact MTs to facilitate intracellular trafficking of DNA repair proteins to the nucleus. As expected, total H2AX protein levels were not affected by drug treatment. The graphs in Fig. 6B quantitate multiple experiments, with γ-H2AX levels normalized to GAPDH, and the starting level arbitrarily set at 1 for the doxorubicin-treated cells (DOX). The plots illustrate the more rapid disappearance of γ-H2AX levels in cells treated only with doxorubicin.

Proteomic Analysis of Dynein Immunoprecipitates Identifies Additional DNA Damage-Repair Protein Candidates. Finally, recognizing that many other proteins are involved in repair of DNA damage, we performed a proteomic analysis of a dynein immunoprecipitate to identify, in a preliminary way, candidate proteins that might also traffic on MTs. The proteins identified are summarized in Table S2. As expected, a diverse group of DNA damage-repair proteins were identified as protein candidates whose trafficking might be impaired, suggesting that impairing MT trafficking is likely to have broad consequences.

Discussion

MTAs, first introduced into the clinic in the late 1950s, are widely used in the therapy of cancer. Given the importance of MTs in cell division and the widely accepted concept that cancer cells divide more rapidly than normal cells, it has been generally assumed that MTAs mediate cytotoxicity by interfering with mitosis (1, 2). Elegant in vitro and preclinical data have demonstrated time and again that MTAs lead to mitotic arrest and in

turn cell death (5, 7–12). Arrest in mitosis as the mechanism that leads to cell death is possible in these preclinical models because their doubling times range from a few hours to at most a few days, and even brief drug exposures are likely to encounter a substantial fraction of cells traversing through mitosis. However, most human tumors have doubling times of 30–60 d or longer (3, 5), making it difficult—indeed almost impossible—to explain how mitotic arrest could be the mechanism of action when MTAs are administered to patients. We have proposed that rather than mitotic arrest, the principal mechanism of action of MTAs in a clinical setting is interference with intracellular trafficking during interphase (3, 4). Key to this concept is identification of the critical proteins whose impaired trafficking on MTs leads to cytotoxicity. A straightforward example is provided by docetaxel and cabazitaxel, the only two "cytotoxic" agents approved in prostate cancer (13, 14). Given the often very indolent nature of prostate cancer, it is difficult to argue that mitotic arrest is the mechanism of action for docetaxel and cabazitaxel in this disease (15–17). Instead, it is increasingly accepted that interference with trafficking of the androgen receptor is the mechanism of action (18, 19), a concept reinforced by the demonstration of tumors previously thought to be "androgen independent" that in fact continue to be very dependent on androgens (20–22).

Considering combinations used in the therapy of a variety of cancers, we realized they frequently included a DDA and a MTA (Table S1). Although this finding might be fortuitous or reflect the drugs available in oncology during the past five decades, the possibility this was other than a chance occurrence intrigued us. Turning to the paradigm that one must identify critical proteins whose function requires intact MTs to explain the efficacy of MTAs in a given cancer, we postulated and set out to prove that the crucial proteins affected by the MTAs in these combinations might be ones involved in DNA repair, and that by inhibiting their trafficking, MTAs could enhance the damage inflicted by the DDA. The data presented unequivocally demonstrate nine proteins involved in the repair of DNA damage associating with dynein and with MTs, and that by interfering with their trafficking, MTAs prolong DNA damage. We thus nominate these nine proteins to what should become a growing list of crucial proteins trafficking on MTs. For some of these proteins (23–26), an association with or trafficking on MTs has been previously reported and the present data corroborate and extend those observations (27).
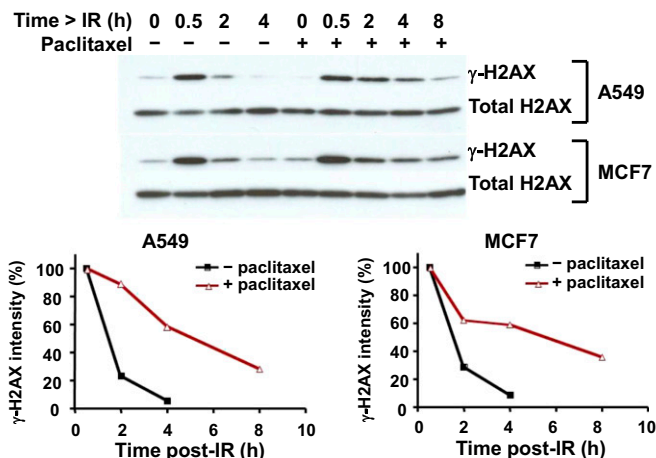

Fig. 5. Addition of paclitaxel treatment to irradiation prolongs γ-H2AX protein detection in A549 and MCF7 cells. Cells were pretreated or not with 200 nM paclitaxel for 24 h, irradiated with 10 Gy, and then further incubated for 0.5, 2, 4, or 8 h before γ-H2AX, a phosphorylated form of H2AX indicating DNA damage, was assessed by immunoblot.
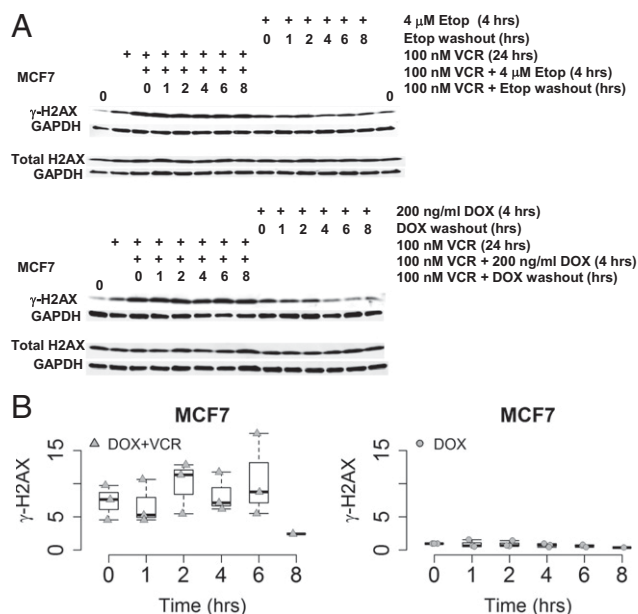
Fig. 6. Addition of vincristine to a DNA-damaging agent prolongs γ-H2AX levels in MCF7 cells. (*A*) MCF7 cells were treated with vincristine (VCR) for 24 h before a 4 h incubation of VCR in combination with either 4 μM etoposide or 200 ng/mL doxorubicin (DDAs) before the DDA was washed out with VCR present for 1, 2, 4, 6, or 8 h. MCF7 cells that had only the DDA treatment for 4 h before its washout were used for comparison. Western blots were probed with antibodies to γ-H2AX, total H2AX, and GAPDH. (*B*) The graphs summarize data from multiple Western blots quantitated for γ-H2AX, normalized to GAPDH. The normalized relative initial γ-H2AX values for the VCR/DOX combination and the DOX washout in the presence of VCR are represented as box plots compared with the DOX treatment alone. The starting level of γ-H2AX was arbitrarily set equal to 1 for the DOX treatment alone, γ-H2AX values for each of the DOX washout time points is expressed in relation to 1 and graphically represented. The triangles and circles represent the observed data points. The white box represents the interquartile range, its bottom the 25th percentile, its top the 75th percentile, the black line the 50th percentile. The whiskers extending from the box do so to the most extreme data point, which is no more than 1.5-times the interquartile range from the box.

We demonstrate effects consistent with our hypothesis using multiple cell lines, different methodologies, and both vincristine and paclitaxel. Cytoplasmic retention of proteins that repair DNA occurs with the addition of vincristine and paclitaxel in adherent A549 and MCF7 cells, as well as four nonadherent Burkitt's lymphoma cell lines and also in SKOV3 cells. That the retention is caused by interfering with MTs and is not a consequence of cell cycle arrest is supported by the results with the AKI (VX680) that achieved similar G_2M arrest but had no effect on the intracellular distribution of the proteins that repair DNA damage. Additionally, taking advantage of the slower transit through the cell cycle that occurs when SKOV3 cells are deprived of serum, we show that despite reducing the number of cells in "mitosis," vincristine still leads to cytoplasmic retention of the DNA damage-repair proteins. Coimmunoprecipitation of the DNA damage-repair proteins with the MT motor protein dynein is consistent with dynein-mediated nuclear trafficking and is supported by the colocalization with tubulin seen by immunofluorescence. We note that, as we have previously shown for p53 (28), association with dynein occurred even in the presence of vincristine, indicating that intact MTs, although essential for trafficking, are not needed for the interaction with dynein that likely occurs in the cytoplasm before "loading" onto MTs. Functionally, the observation that more sustained levels of γ-H2AX are achieved when vincristine or paclitaxel is added to radiation or a DDA provides evidence that

interfering with MT-trafficking can augment DNA damage, given that γ-H2AX is considered a surrogate of the extent of DNA damage (29, 30). This finding then provides a likely explanation for why combinations involving a MTA and a DDA have emerged "empirically" as active combinations in the majority of cancers. Our choice of which proteins involved in the repair of DNA damage to study was guided in large part by the availability of antibodies that worked well on immunoblots or immunofluorescence in A549 cells. Although many of these proteins have been implicated in the repair of radiation, as well as doxorubicin- and etoposide-induced DNA damage (31–34), we do not mean to imply they were all actively involved in the settings we examined. Nevertheless the experiments conducted with vincristine without a DDA, the dynein immunoprecipitation, and the immunolocalization all confirm the importance of intact MTs in intracellular trafficking of these proteins, and their association with MTs as well as dynein, the motor protein responsible for trafficking to the nucleus. Furthermore, we would expect additional proteins would be involved, as shown by our preliminary proteomic analysis.

Fifty years after the introduction of MTAs into clinical oncology, their mechanism of action in human tumors is becoming increasingly clear. To the androgen receptor, we now add numerous proteins involved in the repair of DNA damage as crucial proteins whose function is interdicted by inhibiting trafficking on MTs, resulting in prolonged DNA damage when used in combination with a DDA. We would anticipate that further inquiries should identify additional essential proteins and provide greater insight into tumor biology. Given their central role in the therapy of cancer, MTAs will continue to be used widely in combinations, both with "classic cytotoxic agents" and likely with "targeted therapies." We suggest that to make their use in combinations more rational, one should seek to identify the crucial proteins whose trafficking is disrupted. In this way it may be possible to go beyond additivity and instead reach for synergy.

Materials and Methods

Cell Lines and Reagents. CA46, DG-75, Ramos, ST486 (Burkitt's lymphoma), A549 (lung carcinoma), and MCF7 (breast carcinoma) cell lines were obtained from the American Type Culture Collection. The SKOV3 (ovarian carcinoma) cell line was obtained from the NCI-60 Drug Screen. Doxorubicin, vincristine, and etoposide were purchased from Sigma, and VX-680 (Tozasertib) was obtained from Chemietek.
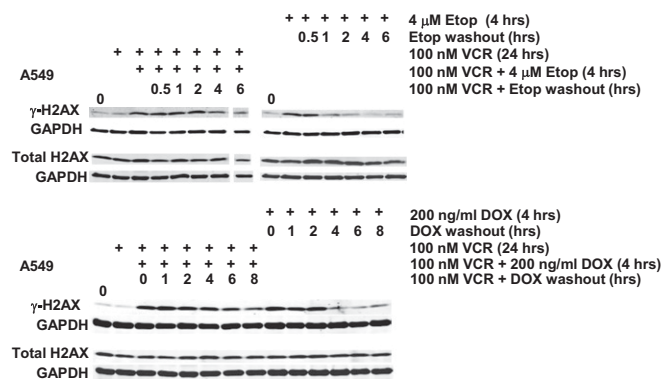

Fig. 7. Addition of vincristine to a DNA-damaging agent prolongs γ-H2AX levels in A549 cells. A549 cells were treated with VCR for 24 h before a 4 h incubation of VCR in combination with either 4 μM etoposide or 200 ng/mL doxorubicin (DDA) before the DDA was washed out with VCR present for 1, 2, 4, 6, or 8 h. A549 cells that had only received the DDA for 4 h before its washout were used for comparison. Western blots were probed with antibodies to γ-H2AX, total H2AX, and GAPDH. The 6-h etoposide washout time-point sample for the VCR/etoposide combination was underloaded, and the bands shown in the offset tracks are from darker exposures.

Protein Analysis in Nuclear and Cytoplasmic Fractions. Nuclear (N) and cytoplasmic (C) fractions were generated according to the protocol of the NE-PER Nuclear and Cytoplasmic Extraction Reagents Kit (Thermo Scientific). Aliquots of whole-cell lysates or 10% of the volume of N or C fractions were separated by SDS/PAGE. Blots were incubated in antibodies discussed in *SI Materials and Methods*. This process was followed by IRDye infrared secondary antibodies (LiCor) and expression quantitated using the Odyssey Infrared Imager (LiCor) (35). The percentage of cytoplasmic retention is indicated and calculated as $[C/(C+N)] \times 100\%$.

Drug Treatment. A549 cells were cultured for 24 h without drug or treated with either vincristine or the AKI VX-680 (Tozasertib) and then treated or not with doxorubicin. SKOV3 cells were cultured in RPMI in the presence or absence of serum for 48 h (6) before treatment with or without 100 nM vincristine for an additional 24 h, with or without serum. Nuclear and cytoplasmic fractions were prepared as described or cells were further processed for flow cytometry (36). Mitotic cells were quantitated by two-variable analysis (37), using an FITC-labeled antiphospho histone H3 (Ser10) antibody (Cell Signaling).

Treatment of Cells with MTA or DDAs and Washout of DNA-Damaging Agent. A549 or MCF7 cells were either pretreated with 100 nM vincristine (VCR) for 24 h before a 4 h treatment with a combination of either VCR and 200 ng/mL doxorubicin or VCR and 4 μM etoposide, followed by washout of the DDA for either 0, 1, 2, 4, 6, or 8 h, in the presence of VCR. Control cells were either untreated or treated with 200 ng/mL doxorubicin or 4 μM etoposide for 4 h before washout of the DDA for identical time periods. Cells were harvested at 4 °C, in 20 mM Tris pH7.5, 150 mM NaCl, 1 mM EDTA, 1% TX-100, with protease (aprotinin, Sigma, and cOmplete Mini, EDTA-free, Roche) and phosphatase inhibitors (PhosSTOP, Roche), frozen, and sonicated before SDS/PAGE. Western blots were probed with antibodies for γ-H2AX, total H2AX, or GAPDH, followed by IRDye infrared secondary antibodies (LiCor) and expression quantitated using the Odyssey Infrared Imager (LiCor) (35).

Immunofluorescence. A549 cells were fixed in either ice-cold 100% methanol for 8 min at −20 °C, or in 4% (vol/vol) paraformaldehyde for 30 min at 22 °C, followed by 100% methanol for 8 min at 20 °C, or in 4% (vol/vol) para-formaldehyde for 15 min at 22 °C, followed by 0.3% TX-100 for 60 min. Cells were processed for immunofluorescence microscopy with modifications of previously described methods (35, 38) and the antibodies used are described in *SI Materials and Methods*.

Dynein Immunoprecipitation. Coimmunoprecipitations in A549 cells were modified from previously described methods (28). Blots were probed with anti-dynein, anti-Bim, and other antibodies as described above. Additional procedures are described in *SI Materials and Methods*.

Proteomics. Cell lysate was immunoprecipitated with anti-dynein conjugated to M-270 Epoxy Dynabeads (Life Technol) and analyzed by mass spectrometry as previously described (39) and described in *SI Materials and Methods*.

1. Milas L, et al. (1995) Kinetics of mitotic arrest and apoptosis in murine mammary and ovarian tumors treated with taxol. *Cancer Chemother Pharmacol* 35(4):297–303.
2. Horton JK, Houghton PJ, Houghton JA (1988) Relationships between tumor responsiveness, vincristine pharmacokinetics and arrest of mitosis in human tumor xenografts. *Biochem Pharmacol* 37(20):3995–4000.
3. Komlodi-Pasztor E, Sackett D, Wilkerson J, Fojo T (2011) Mitosis is not a key target of microtubule agents in patient tumors. *Nat Rev Clin Oncol* 8(4):244–250.
4. Komlodi-Pasztor E, Sackett DL, Fojo AT (2012) Inhibitors targeting mitosis: Tales of how great drugs against a promising target were brought down by a flawed rationale. *Clin Cancer Res* 18(1):51–63.
5. Mitchison TJ (2012) The proliferation rate paradox in antimitotic chemotherapy. *Mol Biol Cell* 23(1):1–6.
6. Shin J-S, et al. (2008) Serum starvation induces G1 arrest through suppression of Skp2-CDK2 and CDK4 in SK-OV-3 cells. *Int J Oncol* 32(2):435–439.
7. Jordan MA, Horwitz SB, Lobert S, Correia JJ (2008) Exploring the mechanisms of action of the novel microtubule inhibitor vinflunine. *Semin Oncol* 35(3, Suppl 3):S6–S12.
8. Oroudjev E, et al. (2010) Maytansinoid-antibody conjugates induce mitotic arrest by suppressing microtubule dynamic instability. *Mol Cancer Ther* 9(10):2700–2713.
9. Yang CP, Liu L, Ikui AE, Horwitz SB (2010) The interaction between mitotic checkpoint proteins, CENP-E and BubR1, is diminished in epothilone B-resistant A549 cells. *Cell Cycle* 9(6):1207–1213.
10. Gan PP, et al. (2010) Microtubule dynamics, mitotic arrest, and apoptosis: Drug-induced differential effects of betaIII-tubulin. *Mol Cancer Ther* 9(5):1339–1348.
11. Rovini A, Savry A, Braguer D, Carré M (2011) Microtubule-targeted agents: When mitochondria become essential to chemotherapy. *Biochim Biophys Acta* 1807(6):679–688.
12. Hage-Sleiman R, Herveau S, Matera EL, Laurier JF, Dumontet C (2011) Silencing of tubulin binding cofactor C modifies microtubule dynamics and cell cycle distribution and enhances sensitivity to gemcitabine in breast cancer cells. *Mol Cancer Ther* 10(2):303–312.
13. de Bono JS, et al.; TROPIC Investigators (2010) Prednisone plus cabazitaxel or mitoxantrone for metastatic castration-resistant prostate cancer progressing after docetaxel treatment: A randomised open-label trial. *Lancet* 376(9747):1147–1154.
14. Tannock IF, et al.; TAX 327 Investigators (2004) Docetaxel plus prednisone or mitoxantrone plus prednisone for advanced prostate cancer. *N Engl J Med* 351(15):1502–1512.
15. Gulley JL, et al. (2010) Immunologic and prognostic factors associated with overall survival employing a poxviral-based PSA vaccine in metastatic castrate-resistant prostate cancer. *Cancer Immunol Immunother* 59(5):663–674.
16. Popiolek M, et al. (2013) Natural history of early, localized prostate cancer: A final report from three decades of follow-up. *Eur Urol* 63(3):428–435.
17. Eichholz A, Ferraldeschi R, Attard G, de Bono JS (2012) Putting the brakes on continued androgen receptor signaling in castration-resistant prostate cancer. *Mol Cell Endocrinol* 360(1-2):68–75.
18. Darshan MS, et al. (2011) Taxane-induced blockade to nuclear accumulation of the androgen receptor predicts clinical responses in metastatic prostate cancer. *Cancer Res* 71(18):6019–6029.
19. Zhu M-L, et al. (2010) Tubulin-targeting chemotherapy impairs androgen receptor activity in prostate cancer. *Cancer Res* 70(20):7992–8002.
20. de Bono JS, et al.; COU-AA-301 Investigators (2011) Abiraterone and increased survival in metastatic prostate cancer. *N Engl J Med* 364(21):1995–2005.
21. Ryan CJ, et al.; COU-AA-302 Investigators (2013) Abiraterone in metastatic prostate cancer without previous chemotherapy. *N Engl J Med* 368(2):138–148.
22. Scher HI, et al.; AFFIRM Investigators (2012) Increased survival with enzalutamide in prostate cancer after chemotherapy. *N Engl J Med* 367(13):1187–1197.
23. Giannakakou P, et al. (2002) Enhanced microtubule-dependent trafficking and p53 nuclear accumulation by suppression of microtubule dynamics. *Proc Natl Acad Sci USA* 99(16):10855–10860.
24. Jang CY, Kim HD, Zhang X, Chang JS, Kim J (2012) Ribosomal protein S3 localizes on the mitotic spindle and functions as a microtubule associated protein in mitosis. *Biochem Biophys Res Commun* 429(1-2):57–62.
25. Suárez-Sánchez R, et al. (2014) Nucleocytoplasmic shuttling of the Duchenne muscular dystrophy gene product dystrophin Dp71d is dependent on the importin α/β and CRM1 nuclear transporters and microtubule motor dynein. *Biochim Biophys Acta* 1843(5):985–1001.
26. Belanto JJ, et al. (2014) Microtubule binding distinguishes dystrophin from utrophin. *Proc Natl Acad Sci USA* 111(15):5723–5728.
27. Thadani-Mulero M, Nanus DM, Giannakakou P (2012) Androgen receptor on the move: Boarding the microtubule expressway to the nucleus. *Cancer Res* 72(18):4611–4615.
28. Trostel SY, Sackett DL, Fojo T (2006) Oligomerization of p53 precedes its association with dynein and nuclear accumulation. *Cell Cycle* 5(19):2253–2259.
29. Kinner A, Wu W, Staudt C, Iliakis G (2008) Gamma-H2AX in recognition and signaling of DNA double-strand breaks in the context of chromatin. *Nucleic Acids Res* 36(17):5678–5694.
30. Solier S, Pommier Y (2014) The nuclear γ-H2AX apoptotic ring: Implications for cancers and autoimmune diseases. *Cell Mol Life Sci* 71(12):2289–2297.
31. Gupta A, et al. (2014) Role of 53BP1 in the regulation of DNA double-strand break repair pathway choice. *Radiat Res* 181(1):1–8.
32. Tanaka T, et al. (2007) Cytometry of ATM activation and histone H2AX phosphorylation to estimate extent of DNA damage induced by exogenous agents. *Cytometry A* 71(9):648–661.
33. Forrest RA, et al. (2012) Activation of DNA damage response pathways as a consequence of anthracycline-DNA adduct formation. *Biochem Pharmacol* 83(12):1602–1612.
34. Mould E, et al. (2014) Identification of dual DNA-PK MDR1 inhibitors for the potentiation of cytotoxic drug activity. *Biochem Pharmacol* 88(1):58–65.
35. Huff LM, Sackett DL, Poruchynsky MS, Fojo T (2010) Microtubule-disrupting chemotherapeutics result in enhanced proteasome-mediated degradation and disappearance of tubulin in neural cells. *Cancer Res* 70(14):5870–5879.
36. Murphy RF, et al. (2012) Retained platinum uptake and indifference to p53 status make novel transplatinum agents active in platinum-resistant cells compared to cisplatin and oxaliplatin. *Cell Cycle* 11(5):963–973.
37. Li PK, et al. (2006) A thalidomide analogue with in vitro antiproliferative, antimitotic, and microtubule-stabilizing activities. *Mol Cancer Ther* 5(2):450–456.
38. Poruchynsky MS, et al. (2008) Proteasome inhibitors increase tubulin polymerization and stabilization in tissue culture cells: A possible mechanism contributing to peripheral neuropathy and cellular toxicity following proteasome inhibition. *Cell Cycle* 7(7):940–949.
39. Guha U, et al. (2008) Comparisons of tyrosine phosphorylated proteins in cells expressing lung cancer-specific alleles of EGFR and KRAS. *Proc Natl Acad Sci USA* 105(37):14112–14117.